*sustainability*

MDPI

*Article*

# Date Palm Waste-Derived Biochar for Improving Hydrological Properties of Sandy Soil Under Saturated and Unsaturated Conditions

**Abdulaziz G. Alghamdi *, Abdulrasoul Alomran, Hesham M. Ibrahim, Arafat Alkhasha and Zafer Alasmary**

Soil Sciences Department, College of Food and Agricultural Sciences, King Saud University, P.O. Box 2460, Riyadh 11451, Saudi Arabia; rasoul@ksu.edu.sa (A.A.); habdou@ksu.edu.sa (H.M.I.); aalkhasha@ksu.edu.sa (A.A.); zalasmari@ksu.edu.sa (Z.A.)

* Correspondence: agghamdi@ksu.edu.sa

**Abstract:** Water conservation and effective irrigation management are vital for sustainable agriculture in arid regions. While organic soil amendments have been widely used to enhance water retention in sandy soils, research on the use of date palm waste-derived biochar remains limited. Thus, this study aimed to explore the innovative application of biochar produced from date palm waste, focusing on its effects on the hydrological properties of sandy soil. Biochars of varying particle sizes (0.5, 1, and 2 mm) and pyrolysis temperatures (300 °C, 450 °C, and 600 °C) were produced and their impacts were assessed under both saturated and unsaturated conditions on soil hydrological properties. The biochar was incorporated into soil columns at application rates of 0%, 1%, 3%, and 5% (*w*/*w*) within a 10 cm layer on top of 35 cm deep soil columns. The soil columns were placed vertically into water basins for saturation. Evaporation, infiltration, and saturated hydraulic conductivity were measured. The findings revealed that the application of 1%, 3%, and 5% biochar significantly increased soil water retention by 36.80%, 34.18%, and 29.66%, while cumulative evaporation decreased by 7.30%, 2.00%, and 1.35%, respectively, as compared to the control. Water retained at the end of the experiment was increased by 100.63%, 112.29%, and 101.68%, while unsaturated hydraulic conductivity decreased by 21.27%, 26.15%, and 26.17% after amending the soil with 1%, 3%, and 5% biochar, respectively, as compared to the control. The water retention ranged between 30.34 and 42.51%, 22.59 and 43.20%, and 22.48 and 38.81% for biochar produced at 300 °C, 450 °C, and 600 °C, respectively. Water infiltration rate and pore size was decreased with the increased pyrolysis temperature. Overall, the application rates of 3% and 5% with particle sizes of 1 and 0.5 mm and low pyrolysis temperature were most efficient for improving soil properties such as water retention, reducing unsaturated hydraulic conductivity, reducing the rate and volume of infiltration, and enhancing the micro-porosity reduction of sandy soils. In a nutshell, this study highlights the potential of date palm waste-derived biochar as an effective soil amendment, significantly enhancing water retention by up to 112.29% and reducing evaporation. By optimizing irrigation management in sandy soils, these findings contribute to more sustainable agricultural practices.

**Keywords:** biochar; evaporation; saturated and unsaturated; water retention; hydraulic conductivity; cumulative infiltration; water savings

check for updates

**Citation:** Alghamdi, A.G.; Alomran, A.; Ibrahim, H.M.; Alkhasha, A.; Alasmary, Z. Date Palm Waste-Derived Biochar for Improving Hydrological Properties of Sandy Soil Under Saturated and Unsaturated Conditions. *Sustainability* **2024**, *16*, 11081. https://doi.org/10.3390/su162411081

Academic Editor: Michael Blanke

Received: 6 November 2024
Revised: 5 December 2024
Accepted: 15 December 2024
Published: 17 December 2024

**Copyright:** © 2024 by the authors. Licensee MDPI, Basel, Switzerland. This article is an open access article distributed under the terms and conditions of the Creative Commons Attribution (CC BY) license (https://creativecommons.org/licenses/by/4.0/).

## 1. Introduction

Sandy soils, covering over 6% of the surface of the globe, are characterized by their coarse texture, low organic matter, and poor nutrient retention, leading to low fertility and suboptimal agricultural productivity [1,2]. To enhance the hydrological properties of these soils, researchers have explored various soil amendments, with biochar emerging as a promising option. Applying soil amendments such as biochar, peat, sewage

sludge, plant residues, and manure could improve the properties of sandy soils, subsequently improving nutrient and water retention [3]. The concept of applying waste-derived biochar as a soil amendment aligns well with the concept of implementing a circular economy for effective waste management. This approach not only reduces waste but also contributes to mitigating climate change and improving crop productivity. The cyclic use of waste products helps achieve economic benefits as well as sustainable agriculture and environment.

Biochar is known to improve soil health by increasing water retention, cation exchange capacity, and nutrient uptake while reducing hydraulic conductivity and evaporation [4,5]. Because of its high energy density, carbon content, and minimal emissions of pollutants, biochar has a lot of promise for energy production. It may effectively produce heat and electricity when used as a solid biofuel in gasification systems, boilers, and internal combustion engines. Furthermore, biochar facilitates the synthesis of synthetic fuel and hydrogen in sophisticated gasification procedures. It is especially useful for off-grid or rural sustainable energy solutions because of its renewable nature and compatibility with decentralized energy systems. Additionally, this multipurpose application fits in nicely with waste management plans. Recent studies have shown that biochar derived from various organic materials can significantly enhance the water retention capacity of sandy soils. For instance, Yost and Hartemink [1] found that biochar from olive waste (leaves and branches) prepared at pyrolytic temperatures of 300 °C, 400 °C, and 500 °C decreased cumulative infiltration, infiltration rate, and cumulative evaporation while increasing available water content. Osman [2] reported that applying poultry litter biochar to soil increased the moisture content and reduced density. In another study, Weber et al. [3] found that biochar particle size affected the hydro-physical properties of surfaces in sandy loam soil. The smallest biochar particle size reduced bulk density and saturated hydraulic conductivity due to increased microporosity, a larger internal surface area, and the porous structure of the biochar particles. Alghamdi [4] reported that applying biochar to sandy soil decreased aeration and the volume of non-capillary pores and increased total porosity, soil moisture, and the volume of capillary pores. Adding fine-sized fractions (below 100 µm) of biochar to soil increased the available water content by 30% compared to untreated soil [6]. Atkinson et al. [5] reported that different biochars (bean harvest residue, corn cobs, and rice husk) improved water content in sandy loam and loamy soils. Alghamdi et al. [7] found a reduced saturated hydraulic conductivity after applying biochar derived from mango twigs and branches at 0, 30, 45, and 60 g $kg^{-1}$ application rates. The biochar was pyrolyzed at 550 °C, mixed with sandy loam and silt loam soils, and subjected to five wetting and drying cycles. Bordoloi et al. [8] found that biochar produced at two different pyrolytic temperatures (400 °C and 500 °C) affected bulk density and water content at field capacity and the permanent wilting point. The available water content was more significant in soil treated with biochar produced at 400 °C than at 500 °C, and this could be related to the fact that the 400 °C biochar was more hydrophilic than the biochar produced at 500 °C. The study reported that applying biochar to the soil as a conditioner increases crop productivity due to enhanced soil structure, aeration, porosity, moisture content, and decreased soil bulk density [9]. Loaiza et al. [10] found that adding 25 g $kg^{-1}$ biochar to silty soil reduced soil bulk density from 1.52 to 1.33 g $cm^{-3}$, improved inter-porosity, and decreased pore radius by 25%. Applying biochar increased saturated hydraulic conductivity in silty sand [10–15]. Alghamdi et al. [16] concluded that the addition of biochar at 4% resulted in a decrease in saturated hydraulic conductivity. In comparison, application at a rate of 8% increased soil moisture content at field capacity and increased stable aggregates in the fraction size 0.25–0.125 mm. Al-Omran et al. [17] reported that adding biochar at a rate of 20 t $ha^{-1}$ without fertilizer application increased bulk density by 12% and plant available water and porosity by 12%. Moreover, Gluba et al. [6] reported that the combined application of biochar and nitrogen fertilizer showed that the biochar treatments improved soil bulk density and total soil porosity at different depths. Gunal et al. [18] reported that this was dependent on soil texture and the feedstock. A sandy soil treated

with biochar showed improved soil properties, such as pore size distribution, air content of the soil, water retention capacity, and soil structure, compared to a sandy soil treated with biochar mixed with farmyard manure at an application rate of 20 t $ha^{-1}$ [19–22]. Thus, adding biochar can be used as a promising amendment to improve the properties of sandy soils, subsequently enhancing their water- and nutrient-holding capacity for better crop production.

Although the benefits of biochar on soil properties are recognized, research on its effects, specifically in sandy soils treated with date palm waste in arid regions, is limited. Moreover, the combined impacts of pyrolytic temperature (300 °C, 450 °C, and 600 °C) and particle size (0.5, 1.0, and 2.0 mm) of date palm waste-derived biochar on the hydrological properties of sandy soils have been least understood. To address these gaps, this study aims to investigate the effects of date palm waste-derived biochar, which is pyrolyzed under different temperature and particle size conditions and applied at various application rates, on the hydrological properties of sandy soil under saturated and unsaturated conditions. This comprehensive assessment of the interactions between biochar properties and sandy soil hydrology is a novel contribution to the existing literature. Thus, it was hypothesized that the application of date palm waste-derived biochar, pyrolyzed at different temperatures (300 °C, 450 °C, and 600 °C) and particle sizes (0.5, 1.0, and 2.0 mm), will significantly improve the hydrological properties of sandy soils under both saturated and unsaturated conditions. The primary objective of this study was to investigate the effects of date palm waste-derived biochar pyrolyzed at different temperatures (300 °C, 450 °C, and 600 °C) with different particle sizes (0.5, 1.0, and 2.0 mm) and application rates (0, 1, 3, and 5% $w/w$) on the hydrological properties of sandy soil under saturated and unsaturated conditions.

## 2. Materials and Methods

### *2.1. Collection and Analyses of Soil and Water Samples*

Soil samples were collected from the surface layer (0–15 cm) of the Agriculture Farm of the College of Food and Agriculture Sciences, King Saud University, located at Deirab (24°250 N, 46°340 E). Soil samples were air-dried and passed through a 2 mm sieve. The chemical and physical properties of the soil were determined according to standard procedures. Soil texture was determined by the hydrometer method [23]. Soil pH was measured using a digital pH meter (WTW pH 315i, Weilheim, Germany) using a saturated soil paste [24]. The electrical conductivity (EC) of the saturated paste extract was measured using a digital EC meter (Jenway 4510 conductivity meter, Stone, Staffordshire, UK). Calcium carbonate was determined using a Calcimeter (Eijkelkamp, Agriearch Equipment, Giesbeek, Gelderland, The Netherlands). Soil organic matter was quantified by the Walkley–Black method reported by [25].

Water samples for the irrigation water were collected and brought to the laboratory. Water was analyzed in the laboratory for salinity, electrical conductivity (EC $dSm^{-1}$ at 25 °C), and pH. Water-soluble sodium ($Na^+$), potassium ($K^+$), magnesium ($Mg^{2+}$), calcium ($Ca^{2+}$), sulfate ($SO_4{}^{2-}$), and chloride ($Cl^-$) were measured by an ion chromatography device (ICS 5000, Thermo, Waltham, MA, USA; while the soluble carbonate ($CO_3{}^{2-}$) and bicarbonate ($HCO_3{}^-$) concentrations were measured by a titration method [26,27]. The chemical characteristics of soil and water are presented in Table 1.

**Table 1.** Chemical properties of soil and water used in this study.

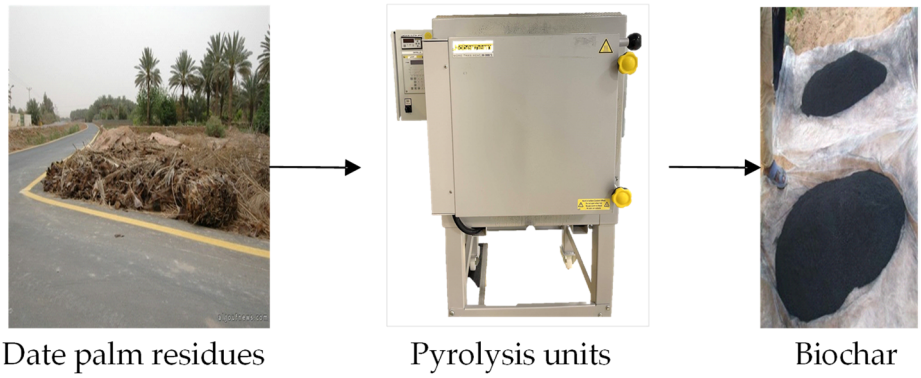
| Parameter | Unit | Soil | Water |
|---|---|---|---|
| pH | -- | 6.46 | 7.07 |
| EC | $dSm^{-1}$ | 1.69 | 1.05 |

**Table 1.** *Cont.*

| Parameter | Unit | Soil | Water |
|---|---|---|---|
| $Ca^{2+}$ | $meq^{-1}$ | 4.67 | 4 |
| $Mg^{2+}$ | | 5.33 | 2.67 |
| $Na^{2+}$ | | 1.32 | 2.6 |
| $K^{+}$ | | 4.83 | 0.19 |
| $Cl^{-}$ | | 2.67 | 6.67 |
| $HCO_3^{-}$ | | 0.27 | 0.27 |
| $CO_3^{2-}$ | | 0 | 0 |
| $SO_4^{2-}$ | | 13.2 | 2.5 |
| Sand | % | 90.83 | -- |
| Silt | % | 7.09 | -- |
| Clay | % | 2.08 | -- |
| Soil texture | -- | Sand | -- |
| Bulk density | $g\ cm^{-3}$ | 1.6 | -- |
| Hydraulic conductivity | $cm\ min^{-1}$ | 0.28 | -- |

### *2.2. Biochar Production and Characterization*

Date palm residues (fronds and rachis) were used as feedstock to produce biochar. The feedstock waste was collected from a local date palm orchard in Riyadh. Collected date palm waste was exposed to direct sunlight to dry out and then cut into small pieces (5–10 cm). These pieces were then placed in a metallic box and subjected to pyrolysis in a muffle furnace (Nabertherm Model 211008, Lilienthal, Germany) and were subjected to pyrolysis at three different temperatures, i.e., 300 °C, 450 °C, and 600 °C, for 4 h at a pyrolysis rate of 10 °C $min^{-1}$. After pyrolysis, the resultant biochar was collected and designated T300, T450, and T600 for the biochar produced at 300 °C, 450 °C, and 600 °C, respectively. Then, the biochar was ground and separated using a mechanical sieve into three parts according to the following order: less than 0.5, 0.5–1.0, and 1–2 mm, designated as P0.5, P1, and P2, respectively. Scheme 1 shows the protocol for biochar production. The biochar was subjected to chemical and elemental analyses, and the results obtained are shown in Table 2. The pH and EC of the produced biochars were determined in a 1:25 ($w/v$) ratio suspension in deionized water. The contents of Ca, Al, Na, and other ions were determined with an ion chromatography device (ICS 5000, Thermo, USA). The elemental composition of the biochar, including C, H, N, and S, was determined using Series II, PerkinElmer, Waltham, MA, USA, while O was estimated using the difference method.




**Scheme 1.** Representation of the transformation of date palm waste into biochar via pyrolysis.

**Table 2.** pH, electrical conductivity, and elemental composition of date palm-derived biochars produced at 300 °C, 450 °C, and 600 °C.

| Parameters | Unit | Biochar 300 °C | Biochar 450 °C | Biochar 600 °C |
|---|---|---|---|---|
| pH (1:25) | -- | 9.38 | 9.42 | 9.66 |
| EC (1:25) | dS $m^{-1}$ | 4.16 | 2.81 | 4.33 |
| C | % | 44.66 | 43.86 | 43.36 |
| N | | 36.55 | 36.55 | 41.85 |
| H | | 3.75 | 2.34 | 3.09 |
| O | | 14.72 | 17.18 | 11.59 |
| S | | 0.32 | 0.07 | 0.11 |
| Na | | 0.19 | 0.63 | 0.02 |
| Mg | | 0.71 | 0.07 | 0.39 |
| Al | | 0.05 | 0.8 | 0.23 |
| Si | | 0.65 | 0.04 | 1.1 |
| Cl | | 0.71 | 0.18 | 0.39 |
| K | | 0.57 | 0.12 | 0.22 |
| Ca | | 0.72 | 0.47 | 0.62 |
| Mn | | 0.14 | 0.02 | 0.11 |

### *2.3. Soil Column Experiment*

#### 2.3.1. Cumulative Evaporation

Soil columns made of transparent plastic were used in this study. The bottoms of the columns were closed using filter paper and a gauze fabric. The columns were 45 mm in internal diameter and 500 mm in height. The columns were packed to a 25 cm depth with 635.85 g of soil, with an average bulk density of 1.6 g $cm^{-3}$ (Figure 1). The biochar mixtures were added in a 10 cm layer over the 25 cm layer of soil. All soil columns were placed vertically into water basins for 2–4 days to ensure saturation by capillary rise up the entire column. All columns were removed from the basins to drain out excess water. After 48 h, columns were weighed to calculate the water retained. Plastic cups were placed at the bottom of each column. The soil columns were placed on a bench inside the laboratory where they were controlled at 22 ± 3 °C and 35 ± 5% relative humidity. Cumulative evaporation was determined daily by weighing each soil column in addition to the water that drained out of each column. All treatments of the experiment are shown in Table 3. At the end of 42 days, each column was divided into six equal sections. The daily measurement of soil column weight was conducted to track cumulative evaporation throughout the experimental period. Furthermore, a daily monitoring of wetting fronts was performed for all the columns.

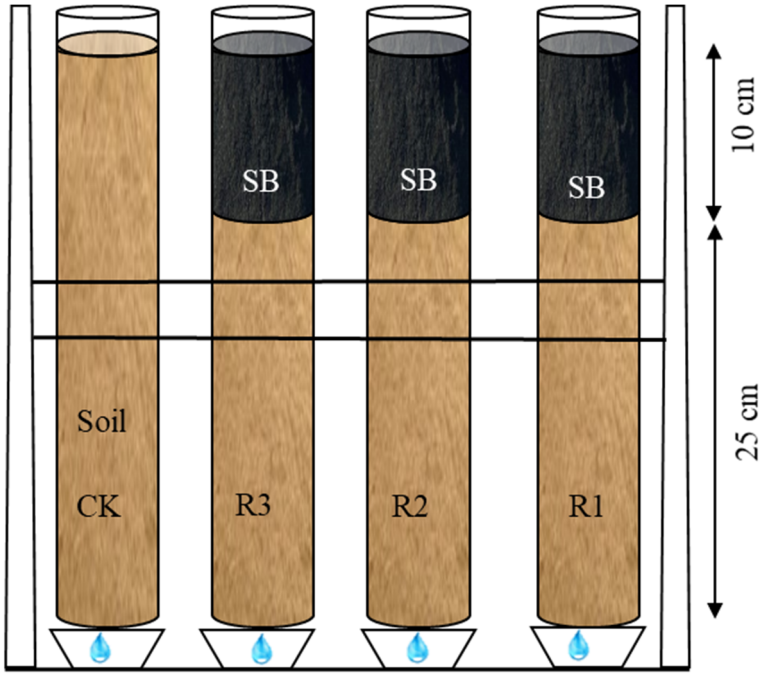
**Table 3.** Details of the treatments with date palm waste biochar produced at 300 °C, 450 °C, and 600 °C.

| Temperature (°C) | Diameter (mm) | Application Rate (%) | Code | Symbol | Replicates |
|---|---|---|---|---|---|
| 300 | 2 | 1 | $T_{300}R_1P_2$ | T1 | 3 |
| | | 3 | $T_{300}R_3P_2$ | T2 | 3 |
| | | 5 | $T_{300}R_5P_2$ | T3 | 3 |
| | 1 | 1 | $T_{300}R_1P_1$ | T4 | 3 |
| | | 3 | $T_{300}R_3P_1$ | T5 | 3 |
| | | 5 | $T_{300}R_5P_1$ | T6 | 3 |
| | 0.5 | 1 | $T_{300}R_1P_{0.5}$ | T7 | 3 |
| | | 3 | $T_{300}R_3P_{0.5}$ | T8 | 3 |
| | | 5 | $T_{300}R_5P_{0.5}$ | T9 | 3 |

**Table 3.** *Cont.*

| Temperature (°C) | Diameter (mm) | Application Rate (%) | Code | Symbol | Replicates |
|---|---|---|---|---|---|
| 450 | 2 | 1 | $T_{450}R_1P_2$ | T10 | 3 |
| | | 3 | $T_{450}R_3P_2$ | T11 | 3 |
| | | 5 | $T_{450}R_5P_2$ | T12 | 3 |
| | 1 | 1 | $T_{450}R_1P_1$ | T13 | 3 |
| | | 3 | $T_{450}R_3P_1$ | T14 | 3 |
| | | 5 | $T_{450}R_5P_1$ | T15 | 3 |
| | 0.5 | 1 | $T_{450}R_1P_{0.5}$ | T16 | 3 |
| | | 3 | $T_{450}R_3P_{0.5}$ | T17 | 3 |
| | | 5 | $T_{450}R_5P_{0.5}$ | T18 | 3 |
| 600 | 2 | 1 | $T_{600}R_1P_2$ | T19 | 3 |
| | | 3 | $T_{600}R_3P_2$ | T20 | 3 |
| | | 5 | $T_{600}R_5P_2$ | T21 | 3 |
| | 1 | 1 | $T_{600}R_1P_1$ | T22 | 3 |
| | | 3 | $T_{600}R_3P_1$ | T23 | 3 |
| | | 5 | $T_{600}R_5P_1$ | T24 | 3 |
| | 0.5 | 1 | $T_{600}R_1P_{0.5}$ | T25 | 3 |
| | | 3 | $T_{600}R_3P_{0.5}$ | T26 | 3 |
| | | 5 | $T_{600}R_5P_{0.5}$ | T27 | 3 |
| CK | | | | CK | 3 |

(T) temperature, (P) particle size, (R) application rate, and (CK) control.




SB= Soil with biochar, R1= 1%, R2= 3% and R3=5%.
CK= untreated soil.

**Figure 1.** A schematic for demonstrating the soil layer with biochar on top of the soil in the treated columns.

2.3.2. Cumulative Infiltration

Infiltration was measured before the saturation process and at the end of 42 days with a mini-disk infiltrometer that held 100 $cm^3$ water (model M11, 0.5 cm suction; Decagon Devices, Pullman, WA, USA). The mini-disk infiltrometer was in complete contact with the soil surface before measurements were taken. The volume of water infiltrated was recorded every 20 s to 200 s. Each treatment was replicated three times. Cumulative infiltration (I) was based on the Philip [28] equation, shown in Equation (1), and the infiltration rate (i) was determined using Equation (2).

$$I = S\sqrt{t} + At \quad (1)$$

where I is the cumulative infiltration (cm), S is the sorptivity ($cm \cdot min^{-0.5}$), and A is a constant related to the hydraulic conductivity. A mathematical representation for Equation (1) was obtained by plotting cumulative infiltration versus the square root of time, and a second-order polynomial was fitted to the measured data.

$$I_i = \frac{1}{2} S_t{}^{-\frac{1}{2}} + A \quad (2)$$

Equation (2) was obtained by plotting cumulative infiltration versus $1/(2\ t^{0.5})$ and fitting a linear equation to the measured data.

2.3.3. Unsaturated Hydraulic Conductivity

Unsaturated hydraulic conductivity K(q) cm $min^{-1}$ for each treatment was calculated with Equation (3).

$$K_{(q)} = \frac{C}{A} \quad (3)$$

where C is the slope of the curve of the cumulative infiltration versus the square root of time, and A is the value in the van Genuchten model related to soil type, suction rate, and radius of the infiltrometer disk and calculated using Equation (4).

$$A = \frac{11.65\left(n^{0.1} - 1\right) exp[2.92(n - 1.9)\alpha h_0]}{(\alpha r_0)^{0.91}}\ n \geq 1.9 \quad (4)$$

where n and $\alpha$ are the van Genuchten parameters for the soil, r0 is the disc radius, and $h_0$ is the suction at the disc surface.

*2.4. Statistical Analysis*

Statistical analyses were carried out using ANOVA, and the least significant difference (LSD at $p < 0.05$) was determined using a software package for Windows (IBM SPSS Statistics 21 Core System, IBM Corporation 2019, Armonk, NY, USA).

## 3. Results and Discussion

*3.1. Water Retention*

The amount of water retained indicated the ability of the biochar treatments to store water in sandy soil. Water retention differed among treatments and depended on the biochar's pyrolytic temperature, application rate, and particle size. The range of percentage increase in water retention ranged between 30.34 and 42.51%, 22.59 and 43.20%, and 22.48 and 38.81% for biochar produced at 300 °C, 450 °C and 600 °C, respectively (Table 4; Appendix A). Previously, Alghamdi et al. [29] reported a significant increase in water retention after biochar application.

CK represents the control, while T1 to T27 represent different treatment schemes. $T_{300}$, $T_{450}$, and $T_{600}$ stand for biochar produced at 300 °C, 450 °C, and 600 °C, respectively. $R_1$, $R_3$, and $R_5$, indicate 1%, 3%, and 5% application rates, respectively. $P_2$, $P_1$, and $P_{0.5}$ show biochar particle sizes of 1–2 mm, 0.5–1.0 mm, and less than 0.5 mm, respectively.

**Table 4.** Cumulative evaporation, water retained, and recovery of all treatments.

| Treatment | Water Saving (mm) | Evaporation (mm) | | | | | | Cumulative Evaporation (mm) | Water Retained (mm) | Recovery % |
|---|---|---|---|---|---|---|---|---|---|---|
| | | Week 1 | Week 2 | Week 3 | Week 4 | Week 5 | Week 6 | | | |
| $T_{300}R_1P_2$ | 134.90 | 24.87 | 16.46 | 12.98 | 13.15 | 12.88 | 6.86 | 87.19 | 46.05 | 98.77 |
| $T_{300}R_3P_2$ | 141.65 | 24.58 | 12.06 | 9.18 | 9.48 | 9.18 | 6.12 | 70.60 | 68.51 | 98.21 |
| $T_{300}R_5P_2$ | 138.27 | 22.29 | 15.64 | 11.97 | 13.46 | 11.89 | 7.84 | 83.10 | 46.05 | 93.40 |
| $T_{300}R_1P_1$ | 130.76 | 24.11 | 16.19 | 13.44 | 13.84 | 14.11 | 7.91 | 89.60 | 27.87 | 89.83 |
| $T_{300}R_3P_1$ | 137.89 | 16.92 | 9.98 | 8.24 | 9.65 | 8.83 | 5.91 | 59.53 | 61.78 | 87.97 |
| $T_{300}R_5P_1$ | 132.92 | 20.30 | 15.18 | 12.14 | 13.17 | 13.71 | 8.43 | 82.93 | 55.04 | 98.52 |
| $T_{300}R_1P_{0.5}$ | 132.53 | 23.36 | 14.51 | 11.93 | 11.76 | 12.62 | 6.69 | 80.88 | 52.40 | 98.85 |
| $T_{300}R_3P_{0.5}$ | 126.40 | 16.48 | 18.91 | 15.14 | 15.94 | 14.32 | 7.55 | 88.34 | 39.19 | 98.45 |
| $T_{300}R_5P_{0.5}$ | 135.82 | 22.88 | 12.25 | 9.12 | 10.76 | 10.40 | 6.44 | 71.84 | 46.05 | 86.80 |
| $T_{450}R_1P_2$ | 129.25 | 21.26 | 14.70 | 12.10 | 11.83 | 13.40 | 6.88 | 80.17 | 46.05 | 97.65 |
| $T_{450}R_3P_2$ | 130.95 | 23.86 | 12.48 | 9.98 | 10.67 | 10.82 | 6.37 | 74.19 | 50.45 | 95.18 |
| $T_{450}R_5P_2$ | 139.34 | 25.02 | 13.80 | 10.67 | 11.74 | 11.34 | 6.14 | 78.72 | 57.75 | 97.94 |
| $T_{450}R_1P_1$ | 133.11 | 19.27 | 13.23 | 9.83 | 9.90 | 10.02 | 5.72 | 67.98 | 46.49 | 86.00 |
| $T_{450}R_3P_1$ | 142.34 | 20.07 | 13.88 | 11.30 | 10.97 | 11.16 | 5.60 | 72.97 | 65.17 | 97.05 |
| $T_{450}R_5P_1$ | 133.24 | 22.06 | 17.47 | 13.13 | 14.53 | 13.57 | 6.04 | 86.79 | 46.05 | 99.70 |
| $T_{450}R_1P_{0.5}$ | 121.85 | 18.35 | 14.51 | 11.37 | 11.43 | 11.22 | 5.35 | 72.22 | 47.31 | 98.09 |
| $T_{450}R_3P_{0.5}$ | 139.11 | 19.27 | 16.21 | 12.16 | 12.88 | 11.87 | 4.32 | 76.71 | 51.21 | 91.92 |
| $T_{450}R_5P_{0.5}$ | 130.89 | 17.30 | 13.76 | 10.55 | 11.05 | 11.62 | 4.76 | 69.03 | 58.19 | 97.09 |
| $T_{600}R_1P_2$ | 132.42 | 18.12 | 13.13 | 10.27 | 11.16 | 11.91 | 6.33 | 70.92 | 56.37 | 96.12 |
| $T_{600}R_3P_2$ | 136.47 | 18.31 | 14.93 | 10.59 | 12.33 | 12.48 | 6.02 | 74.65 | 50.26 | 91.53 |
| $T_{600}R_5P_2$ | 137.98 | 19.82 | 11.62 | 8.72 | 10.53 | 9.75 | 5.14 | 65.57 | 68.63 | 97.26 |
| $T_{600}R_1P_1$ | 126.93 | 20.36 | 13.04 | 9.42 | 10.99 | 11.16 | 5.70 | 70.67 | 55.30 | 98.33 |
| $T_{600}R_3P_1$ | 124.26 | 21.75 | 16.27 | 10.36 | 12.06 | 11.83 | 5.79 | 78.05 | 44.85 | 98.90 |
| $T_{600}R_5P_1$ | 128.10 | 21.01 | 13.90 | 10.36 | 12.06 | 11.83 | 5.79 | 74.94 | 47.68 | 95.73 |
| $T_{600}R_1P_{0.5}$ | 122.10 | 19.75 | 14.01 | 10.67 | 11.28 | 11.37 | 6.75 | 73.83 | 43.34 | 95.96 |
| $T_{600}R_3P_{0.5}$ | 121.75 | 17.95 | 13.88 | 9.98 | 11.09 | 10.36 | 6.88 | 70.14 | 46.36 | 95.69 |
| $T_{600}R_5P_{0.5}$ | 123.78 | 22.40 | 20.47 | 16.10 | 16.54 | 13.23 | 6.96 | 95.70 | 32.46 | 99.59 |
| CK | 82.85 | 22.71 | 19.31 | 11.68 | 8.64 | 7.13 | 4.47 | 73.94 | 24.53 | 99.07 |
| LSD $_{0.05}$ | 0.936 | 0.667 | 0.506 | 0.436 | 0.743 | 0.488 | 0.467 | 0.932 | 0.765 | 0.956 |

CK represents control, while T1 to T27 represent different treatments. $T_{300}$, $T_{450}$, and $T_{600}$ for biochar.

### *3.2. Influence of Pyrolytic Temperature on Cumulative Evaporation*

The influence of biochar produced at different pyrolytic temperatures on cumulative evaporation and water retention is shown in Table 4 and Figure 2. The total amounts of water absorbed by the soil columns differed due to the biochar treatments. Biochar produced at 300 °C increased cumulative evaporation in treatments T1, T3, T4, T6, T7, and T8, and the increase was in the range of 9.39% to 21.19%. In the other treatments, the cumulative evaporation was decreased. Compared to the untreated soil, the highest cumulative evaporation was obtained with treatments T4 ($T_{300}R_1P_1$), T8 ($T_{300}R_3P_{0.5}$), and T1 ($T_{300}R_1P_2$) with the application of the biochar with a particle size of 1, 0.5, and 2 mm and application rates of 1% and 3% (T4, T8, and T1). In addition, cumulative evaporation decreased by 2.84%, 4.51%, and 19.48% for treatments T9 ($T_{300}R_5P_{0.5}$), T2 ($T_{300}R_3P_2$), and T5 ($T_{300}R_3P_1$). These results suggest that, depending on the particle size and application rate, higher application rates of biochar could have partially closed the pores of the sandy soil [29]. The soil moisture was increased by 29.10%, 59.47%, 29.10%, 4.51%, 50.37%, 41.26%, 37.69%, 19.82%, and 29.10% after applying T1 to T9, respectively.

The highest water retention was observed with the biochar application rate of 3% (*w*/*w*). Recovery as a percentage was 98.85%, 98.77%, 98.52%, 98.45%, 98.21%, 93.40%, 89.83%, 87.97%, and 86.80% for T7, T1, T6, T8, T2, T3, T4, T5, and T9, respectively. The highest recovery was observed for T2 ($T_{300}R_3P_2$), followed by T7 ($T_{300}R_1P_{0.5}$), which could be due to a decrease in bulk density as well as an increase in the porosity, which depended on the application rate and the particle size of the biochar [16,30]. Applying biochar might have increased the volume of small pores and enhanced soil aggregation, which resulted in more available water [31]. The cumulative evaporation for biochar produced at 450 °C is shown in Table 4 and Figure 3. The cumulative evaporation was increased by 0.34%, 3.74%, 6.47%, 8.42%, and 17.39% for T11, T17, T12, T10, and T15, respectively. Moreover, the

cumulative evaporation decreased by 1.30%, 2.33%, 6.64%, and 8.05% when applying T14, T16, T18, and T13, respectively, compared with the control. Water content in the columns was increased by 87.69%, 105.64%, 135.38%, 89.49%, 165.64%, 87.69%, 92.82%, 108.72%, and 137.18% with the application of T10 to T18, respectively, compared with the control. The highest water content was found in T14, T18, and T12 ($T_{450}R_3P_1$, $T_{450}R_5P_{0.5}$, and $T_{450}R_5P_2$) with 3% and 5% application rates. Water recovery values were 97.65%, 95.18%, 97.94%, 86.00%, 97.05%, 99.70%, 98.09%, 91.92%, and 97.09% for treatments T10 to T18, respectively. Applying biochar at the highest rate of addition (3% and 5%) produced the best water recovery, according to the water recovery data [16,32,33].

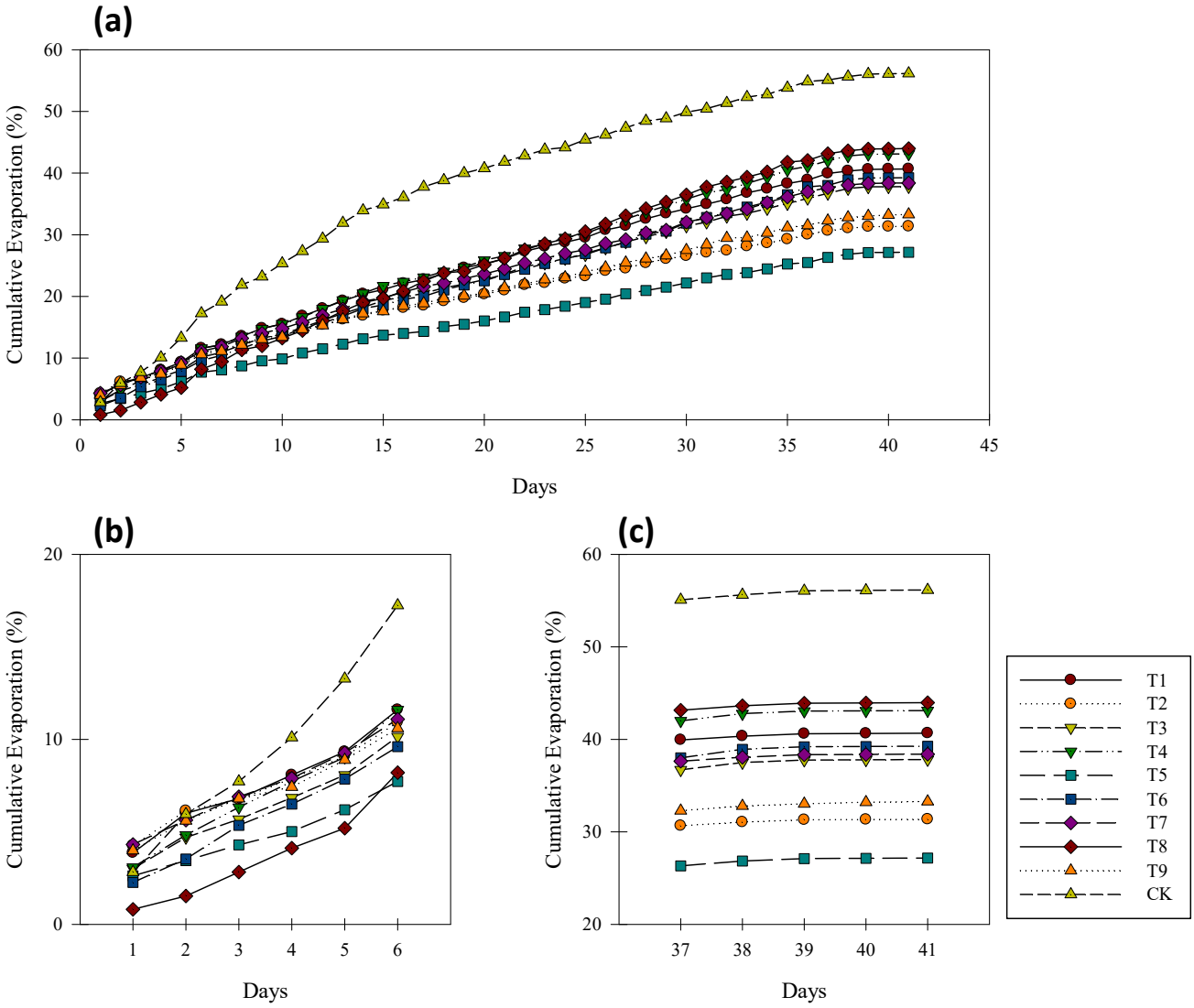



**Figure 2.** Effect of pyrolytic temperature on cumulative evaporation after the application of date palm-derived biochar produced at 300 °C (T300) with particle sizes of 1–2 mm, 0.5–1.0 mm, and less than 0.5 mm (P2, P1, and P0.5, respectively), and applied at 1%, 3%, and 5% (R1, R3, and R5, respectively), with (**a**) showing cumulative evaporation from day 1 to 45, (**b**) showing cumulative evaporation from day 1 to 6, and (**c**) showing cumulative evaporation from day 37 to 41. (CK: Control, T1: $T_{300}R_1P_2$, T2: $T_{300}R_3P_2$, T3: $T_{300}R_5P_2$, T4: $T_{300}R_1P_1$, T5: $T_{300}R_3P_1$, T6: $T_{300}R_5P_1$, T7: $T_{300}R_1P_{0.5}$, T8: $T_{300}R_3P_{0.5}$, and T9: $T_{300}R_5P_{0.5}$).

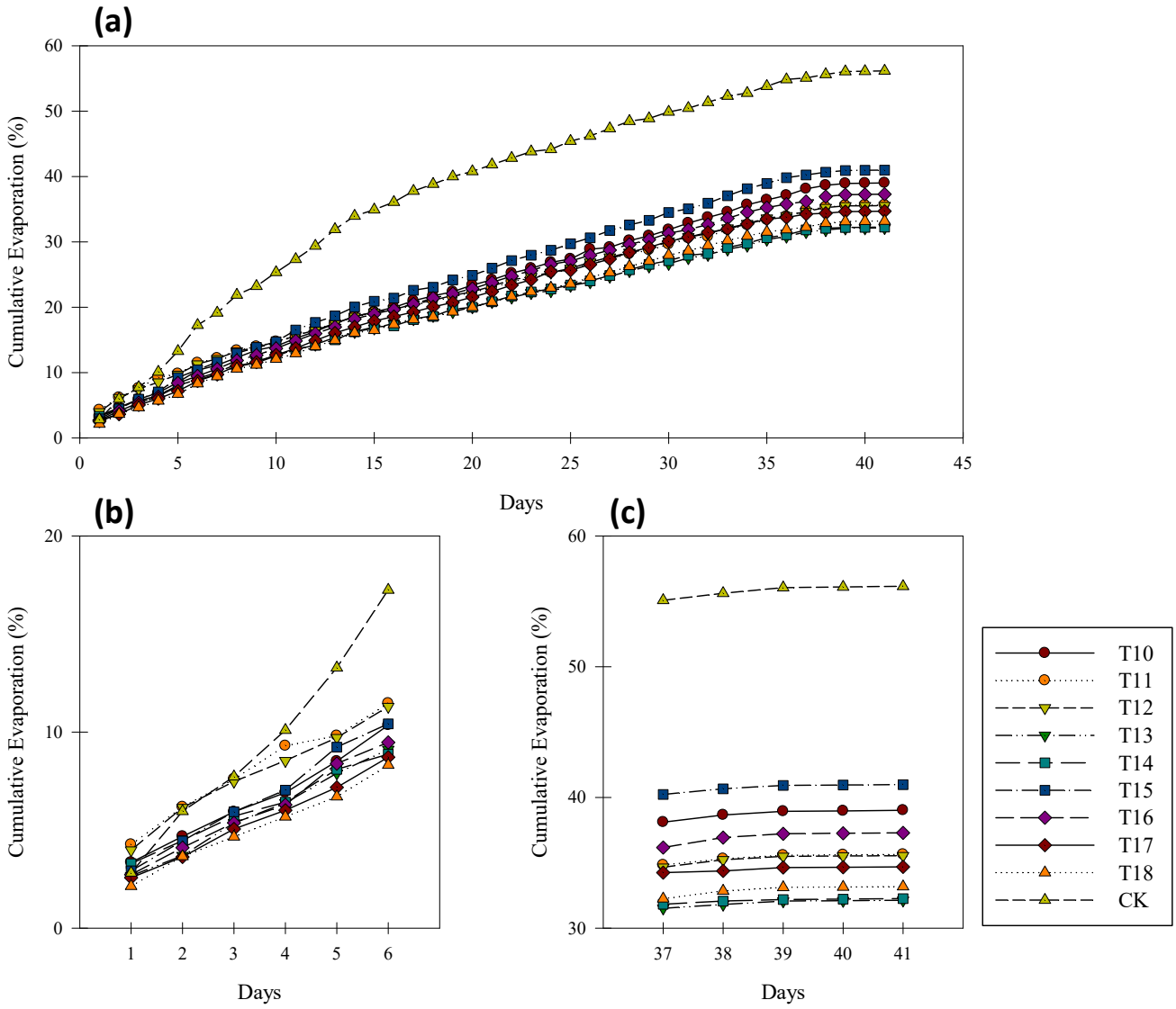



**Figure 3.** Effect of pyrolytic temperature on cumulative evaporation after the application of date palm-derived biochar produced at 300 °C (T300) with particle sizes of 1–2 mm, 0.5–1.0 mm, and less than 0.5 mm (P2, P1, and P0.5, respectively), and applied at 1%, 3%, and 5% (R1, R3, and R5, respectively), with (**a**) showing cumulative evaporation from day 1 to 45, (**b**) showing cumulative evaporation from day 1 to 6, and (**c**) showing cumulative evaporation from day 37 to 41. (CK: Control, T10: $T_{450}R_1P_2$, T11: $T_{450}R_3P_2$, T12: $T_{450}R_5P_2$, T13: $T_{450}R_1P_1$, T14: $T_{450}R_3P_1$, T15: $T_{450}R_5P_1$, T16: $T_{450}R_1P_{0.5}$, T17: $T_{450}R_3P_{0.5}$, and T18: $T_{450}R_5P_{0.5}$).

Cumulative evaporation with biochar produced at 600 °C (Table 4 and Figure 4) increased in treatments T20, T23, T24 and T27, and decreased by 12.31%, 34.10%, 13.33%, 0.43%, and 15.47% in treatments T19, T21, T22, T25, and T26, respectively, compared with the untreated soil. Soil water content was increased by 129.74%, 104.87%, 179.74%, 125.38%, 82.82%, 94.36%, 76.67%, 88.97%, and 32.31% with treatments T19 to T27, respectively, compared to the control. All biochar treatments increased the soil's ability to store water, demonstrating that water retention was influenced by the biochar's pyrolytic temperature, particle size, and application rate. [14,27,33,34]. The significantly highest amount of water content in the soil was observed when applying T21 ($T_{600}R_5P_2$). The increase in cumulative evaporation in most treatments could be attributed to modifying large pore spaces because fine soil filled them. Hence, the pores were blocked or partly clogged,

leading to high evaporation, especially because the biochar was in the top 10 cm of the soil column [17,30,34].

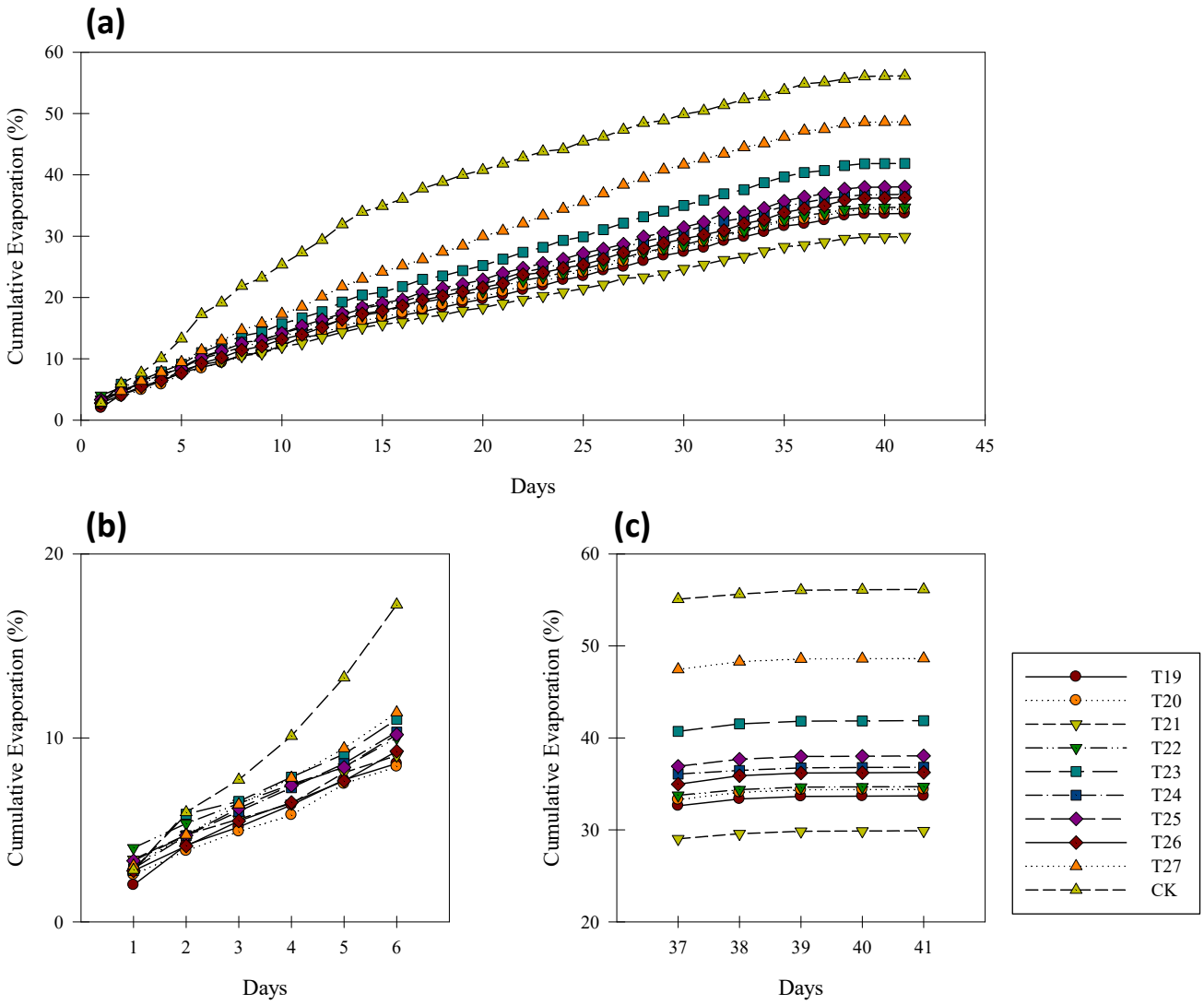



**Figure 4.** Effect of pyrolytic temperature on cumulative evaporation after the application of date palm-derived biochar produced at 300 °C (T300) with particle sizes of 1–2 mm, 0.5–1.0 mm, and less than 0.5 mm (P2, P1, and P0.5, respectively), and applied at 1%, 3%, and 5% (R1, R3, and R5, respectively), with (**a**) showing cumulative evaporation from day 1 to 45, (**b**) showing cumulative evaporation from day 1 to 6, and (**c**) showing cumulative evaporation from day 37 to 41. (CK: Control, T19: $T_{600}R_1P_2$, T20: $T_{600}R_3P_2$, T21: $T_{600}R_5P_2$, T22: $T_{600}R_1P_1$, T23: $T_{600}R_3P_1$, T24: $T_{600}R_5P_1$, T25: $T_{600}R_1P_{0.5}$, T26: $T_{600}R_3P_{0.5}$, and T27: $T_{600}R_5P_{0.5}$).

### *3.3. Interaction of Particle Size and Application Rate of Biochar*

Application rates of biochar produced at various pyrolytic temperatures affected the cumulative evaporation. The different rates applied to the soil columns led to changes in evaporation, and the cumulative evaporation increased on average by 16.17%, 7.24%, 5.74%, and 6.49% for rates 1% and 5% at 300 °C, 5% at 450 °C, and 5% at 600 °C. Cumulative evaporation decreased by 1.5%, 0.65%, and 2.88% for rates 3% and 1% for pyrolytic temperatures at 450 °C, and 1% at 600 °C, respectively, as compared to the control. Furthermore, the impact of the particle size of the biochar affected cumulative evaporation, which increased by 8.60%, 4.62%, and 8.68% for P2, P1, and P0.5 (mm), respectively, for biochar produced at a pyrolytic temperature of 300 °C. In contrast to the control, cumulative evaporation increased by 5.08%, 2.68%, and 8.05% for P2, P1, and P0.5, and reduced by 1.74% and 4.81%

for P0.5 and P2 with biochar at 450 °C and 600 °C. Moreover, the effect of application rate on the water retained in the columns was increased by 71.62%, 130.26%, 99.91%, 90.00%, 126.67%, 120.09%, 110.60%, 92.22%, and 102.14% for rates 1%, 3%, and 5% (*w*/*w*) with biochar pyrolyzed at temperatures of 300 °C, 450 °C, and 600 °C, respectively, compared with untreated soil.

The influences of particles the size of the biochar on water retention increased by 118.21%, 96.58%, 87.01%, 109.57%, 114.27%, 112.91%, 138.12%, 100.85%, and 65.98%, for P2, P1, and P0.5 with biochar pyrolyzed at temperatures of 300 °C, 450 °C, and 600 °C compared with untreated soil.

Our findings exhibited that the application rates of 3% and 5% (*w*/*w*) and 1 and 0.5 mm particles resulted in greater water retention. Previously, it was reported that cumulative evaporation was reduced by 29.27% and 14.61% when biochar was added at higher rates of 4% and 8%, respectively [16]. This could be due to the reduced macrospores of the sandy soil they studied. The study by Šimanský et al. [35] provides further insights into the relationship between biochar application and soil pore characteristics. They found that the reduction in soil pores was correlated with the biochar application rate, suggesting a dose-dependent effect. Additionally, their analysis revealed that the biochar application rate and the biochar particle size influenced certain pore fractions. This indicates that the biochar's quantity and physical properties can modify the soil pore system. The findings from Sun et al. [36] reinforce earlier observations, indicating that the application of biochar can significantly enhance soil physical properties, including aggregate stability, pore-space characteristics, and water retention. Sandy soils, often characterized by poor physical qualities, stand to gain the most from these improvements. Collectively, these studies illustrate the diverse impacts of biochar on soil physical characteristics.

### *3.4. Effect of Biochar on Cumulative Infiltration and Infiltration Rate*

Figure 5 shows cumulative infiltration as affected by the application of biochar with different particle sizes and application rates. The results showed that the cumulative infiltration decreased with biochar application, where the percent decrease was 1.48%, 1.64%, 0.33%, 1.26%, 2.57%, 2.46%, 4.15%, and 5.0% with the application of T2 to T9, respectively, as compared to the control. The highest decreases were found in treatments T9, T8, and T6, and all of these treatments had the fine particle size P (0.5 mm), and the rates of addition were 3% and 5% with a pyrolytic temperature of 300 °C.

Biochar with a pyrolytic temperature of 450 °C caused a decrease in the cumulative infiltration, and it was 0.44%, 1.97%, 1.39%, 2.19%, 2.30%, 4.43%, and 4.75% for treatments T11 to T18, respectively (excluding T13). However, the cumulative infiltration decreased by 0.93%, 1.80%, 1.80%, 2.95%, −2.19%, 4.04%, and 4.92% for treatments T20 to T27, respectively, except for T19 to T22 with a pyrolytic temperature 600 °C. The infiltration rate for all treatments, shown in Figure 6, decreased due to biochar application to the soil. The decrease was lowest for the large particle size of 2 mm, while the highest decrease was found for the fine particle size of 0.5 mm and high biochar application rates (3% and 5%), compared with non-treated soil. The percentage decreased by 1.48%, 1.64%, 0.33%, 1.26%, 2.57%, 2.46%, 4.15%, and 5.00% for treatments T2 to T9, in which the pyrolytic temperature was 300 °C [16,37].

For biochar produced at 450 °C, the decrease in infiltration rate was 0.44%, 1.97%, 1.39%, 2.19%, 2.30%, 4.43%, and 4.75% for treatments T10 to T18 (excluding T13). Furthermore, for biochar prepared at 600 °C, the infiltration rate was reduced by 0.49%, 0.93%, 1.80%, 0.16%, 1.80%, 2.95%, 2.19%, 4.04%, and 4.92% for treatments T19 to T27, respectively, compared with the control. Figures 7 and 8 show cumulative evaporation and infiltration rate data after wetting periods. Cumulative evaporation decreased before and after the periods and ranged between 5.17% and 112.50%, 3.62% and 77.78%, and 16.22% and 96.77% for 300 °C, 450 °C, and 600 °C, respectively. The infiltration rate decreased from 57.76% to 218.75%, 55.43% to 166.67%, and 74.32 to 195.16% for 300 °C, 450 °C, and 600 °C, respectively. The highest reduction in infiltration rate was observed before and after

the experiment duration due to moisture in the soil [27,37]. The observed results could be attributed to the fine particles present in the biochar. These fine particles may have filled or clogged the soil's macropores, reducing the pathways for water conduction. However, under these conditions, water in the root zone would be less prone to deep percolation losses. As a result, more water would be available for plant growth, as suggested by the cited references [38–40].

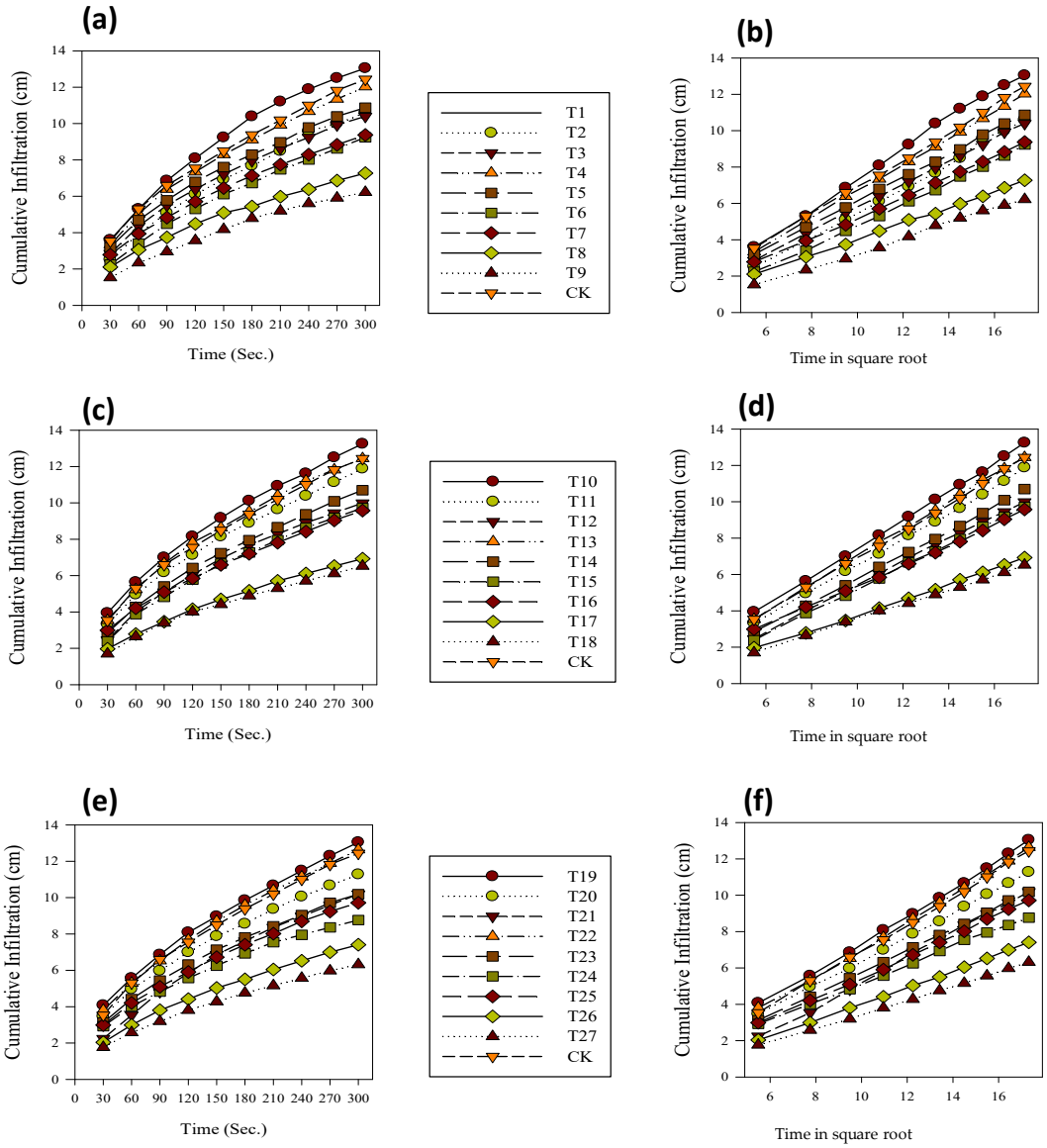



**Figure 5.** Effect of pyrolytic temperature on cumulative infiltration before wetting after the application of date palm-derived biochar produced at 300 °C ($T_{300}$), 450 °C ($T_{450}$), and 600 °C ($T_{600}$) with particle sizes of 1–2 mm, 0.5–1.0 mm, and less than 0.5 mm ($P_2$, $P_1$, and $P_{0.5}$, respectively), and applied at 1%, 3%, and 5% ($R_1$, $R_3$, and $R_5$, respectively). Panel (**a**) shows the plot of cumulative infiltration vs. time, while (**b**) shows the plot of cumulative infiltration vs. sq. time for treatments T1 to T9. Panel (**c**) shows the plot of cumulative infiltration vs. time, while (**d**) shows the plot of cumulative infiltration vs. sq. time for treatments T10 to T18. Panel (**e**) shows the plot of cumulative infiltration vs. time, while (**f**) shows the plot of cumulative infiltration vs. sq. time for treatments T19 to T27. (CK: Control, T1: $T_{300}R_1P_2$, T2: $T_{300}R_3P_2$, T3: $T_{300}R_5P_2$, T4: $T_{300}R_1P_1$, T5: $T_{300}R_3P_1$, T6: $T_{300}R_5P_1$, T7: $T_{300}R_1P_{0.5}$, T8: $T_{300}R_3P_{0.5}$, T9: $T_{300}R_5P_{0.5}$, T10: $T_{450}R_1P_2$, T11: $T_{450}R_3P_2$, T12: $T_{450}R_5P_2$, T13: $T_{450}R_1P_1$, T14: $T_{450}R_3P_1$, T15: $T_{450}R_5P_1$, T16: $T_{450}R_1P_{0.5}$, T17: $T_{450}R_3P_{0.5}$, T18: $T_{450}R_5P_{0.5}$, T19: $T_{600}R_1P_2$, T20: $T_{600}R_3P_2$, T21: $T_{600}R_5P_2$, T22: $T_{600}R_1P_1$, T23: $T_{600}R_3P_1$, T24: $T_{600}R_5P_1$, T25: $T_{600}R_1P_{0.5}$, T26: $T_{600}R_3P_{0.5}$, and T27: $T_{600}R_5P_{0.5}$).

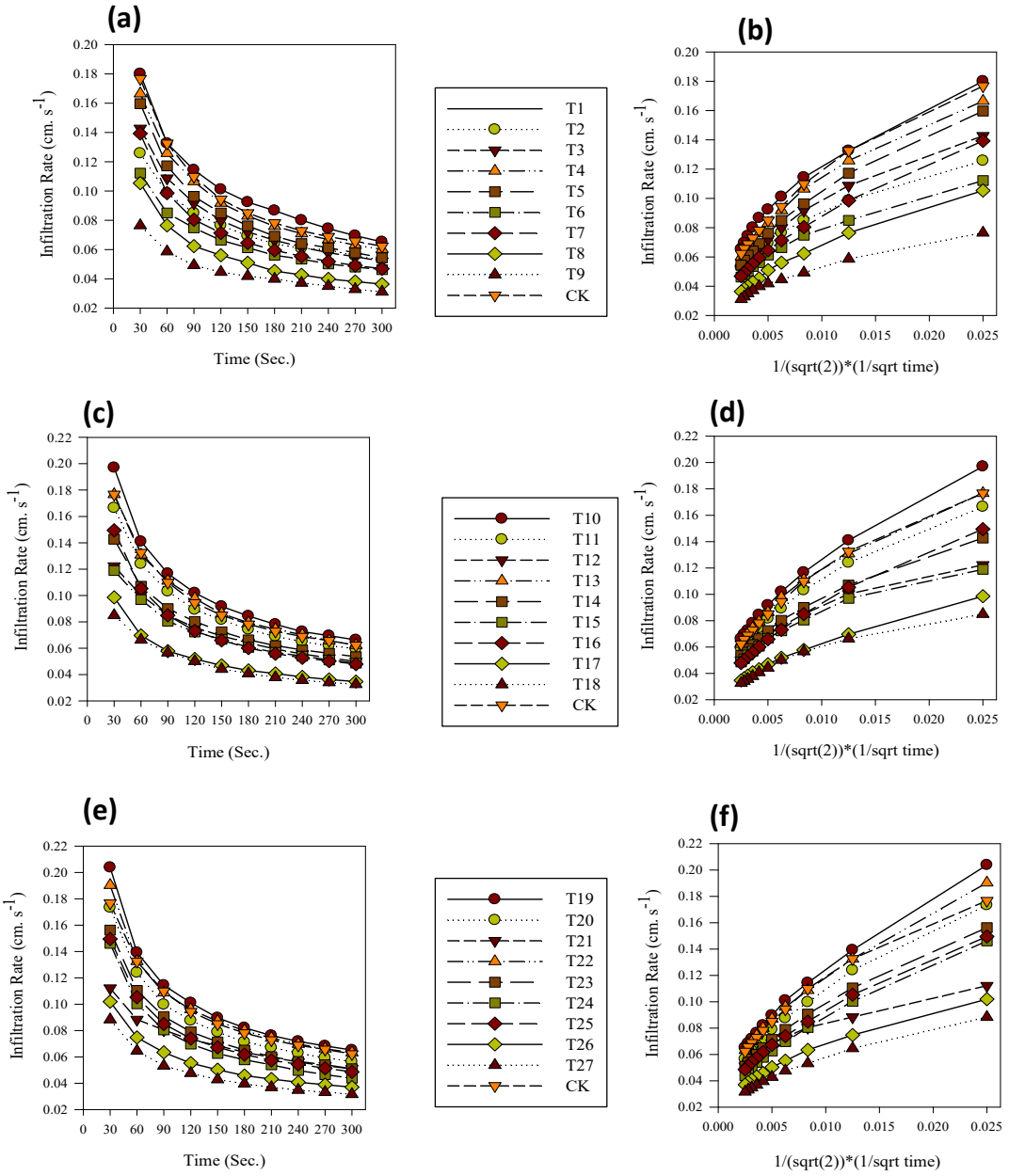



**Figure 6.** Effect of pyrolytic temperature on infiltration rate before wetting after the application of date palm-derived biochar produced at 300 °C ($T_{300}$), 450 °C ($T_{450}$), and 600 °C ($T_{600}$) with particle sizes of 1–2 mm, 0.5–1.0 mm, and less than 0.5 mm ($P_2$, $P_1$, and $P_{0.5}$, respectively), and applied at 1%, 3%, and 5% ($R_1$, $R_3$, and $R_5$, respectively). Panels (**a**,**b**) show the effects of treatments T1 to T9 on the infiltration rate, panels (**c**,**d**) show the effects of treatments T10 to T18 on the infiltration rate, and panels (**e**,**f**) show the effects of treatments T19 to T27 on the infiltration rate (CK: Control, T1: $T_{300}R_1P_2$, T2: $T_{300}R_3P_2$, T3: $T_{300}R_5P_2$, T4: $T_{300}R_1P_1$, T5: $T_{300}R_3P_1$, T6: $T_{300}R_5P_1$, T7: $T_{300}R_1P_{0.5}$, T8: $T_{300}R_3P_{0.5}$, T9: $T_{300}R_5P_{0.5}$, T10: $T_{450}R_1P_2$, T11: $T_{450}R_3P_2$, T12: $T_{450}R_5P_2$, T13: $T_{450}R_1P_1$, T14: $T_{450}R_3P_1$, T15: $T_{450}R_5P_1$, T16: $T_{450}R_1P_{0.5}$, T17: $T_{450}R_3P_{0.5}$, T18: $T_{450}R_5P_{0.5}$, T19: $T_{600}R_1P_2$, T20: $T_{600}R_3P_2$, T21: $T_{600}R_5P_2$, T22: $T_{600}R_1P_1$, T23: $T_{600}R_3P_1$, T24: $T_{600}R_5P_1$, T25: $T_{600}R_1P_{0.5}$, T26: $T_{600}R_3P_{0.5}$, and T27: $T_{600}R_5P_{0.5}$).

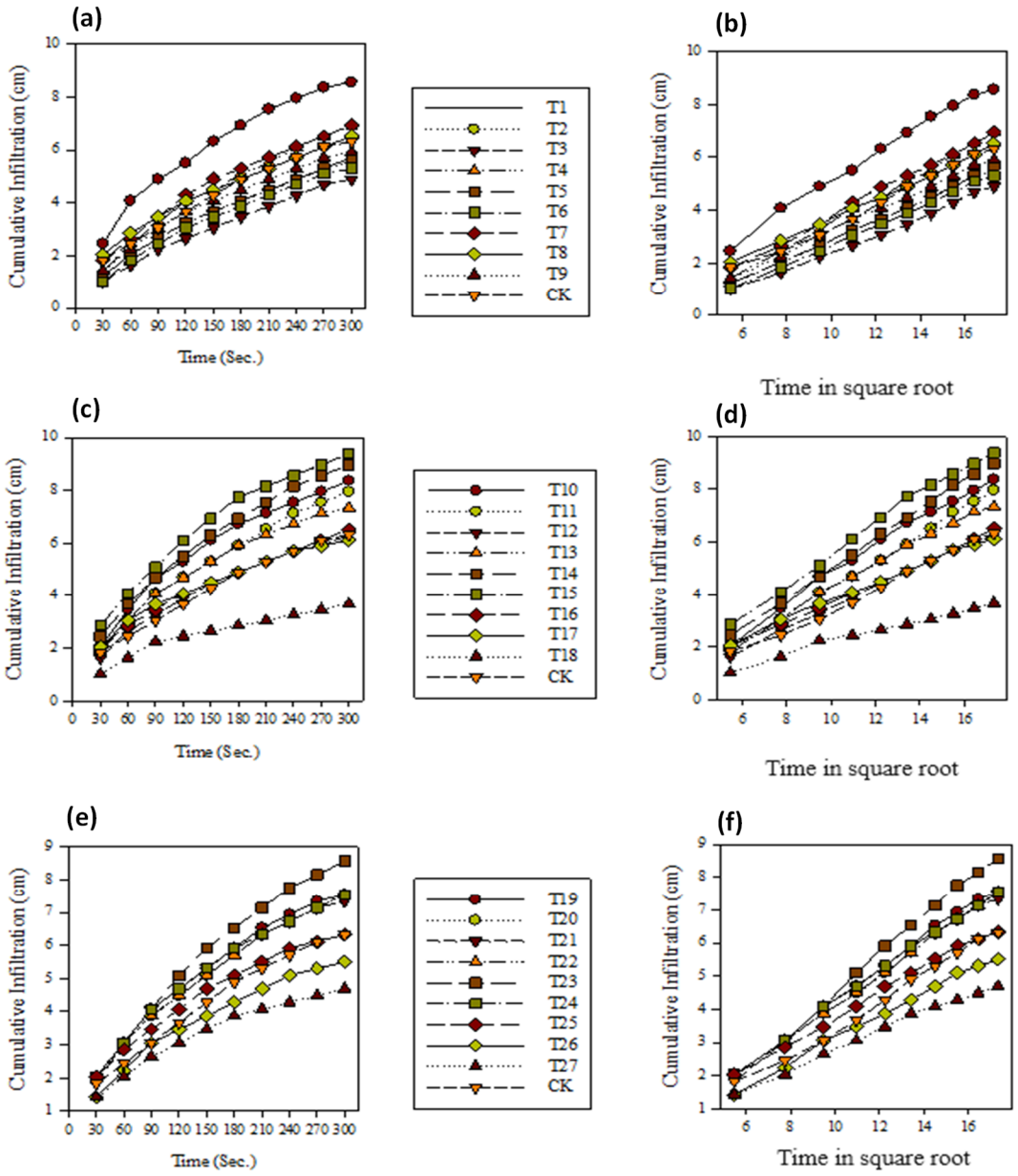



**Figure 7.** Effect of pyrolytic temperature on cumulative infiltration after wetting after the application of date palm-derived biochar produced at 300 °C ($T_{300}$), 450 °C ($T_{450}$), and 600 °C ($T_{600}$) with particle sizes of 1–2 mm, 0.5–1.0 mm, and less than 0.5 mm ($P_2$, $P_1$, and $P_{0.5}$, respectively), and applied at 1%, 3%, and 5% ($R_1$, $R_3$, and $R_5$, respectively). Panels (**a**,**b**) show the effects of treatments T1 to T9 on cumulative infiltration, panels (**c**,**d**) show the effects of treatments T10 to T18 on cumulative infiltration, and panels (**e**,**f**) show the effects of treatments T19 to T27 on cumulative infiltration (CK: Control, T1: $T_{300}R_1P_2$, T2: $T_{300}R_3P_2$, T3: $T_{300}R_5P_2$, T4: $T_{300}R_1P_1$, T5: $T_{300}R_3P_1$, T6: $T_{300}R_5P_1$, T7: $T_{300}R_1P_{0.5}$, T8: $T_{300}R_3P_{0.5}$, T9: $T_{300}R_5P_{0.5}$, T10: $T_{450}R_1P_2$, T11: $T_{450}R_3P_2$, T12: $T_{450}R_5P_2$, T13: $T_{450}R_1P_1$, T14: $T_{450}R_3P_1$, T15: $T_{450}R_5P_1$, T16: $T_{450}R_1P_{0.5}$, T17: $T_{450}R_3P_{0.5}$, T18: $T_{450}R_5P_{0.5}$, T19: $T_{600}R_1P_2$, T20: $T_{600}R_3P_2$, T21: $T_{600}R_5P_2$, T22: $T_{600}R_1P_1$, T23: $T_{600}R_3P_1$, T24: $T_{600}R_5P_1$, T25: $T_{600}R_1P_{0.5}$, T26: $T_{600}R_3P_{0.5}$, and T27: $T_{600}R_5P_{0.5}$).

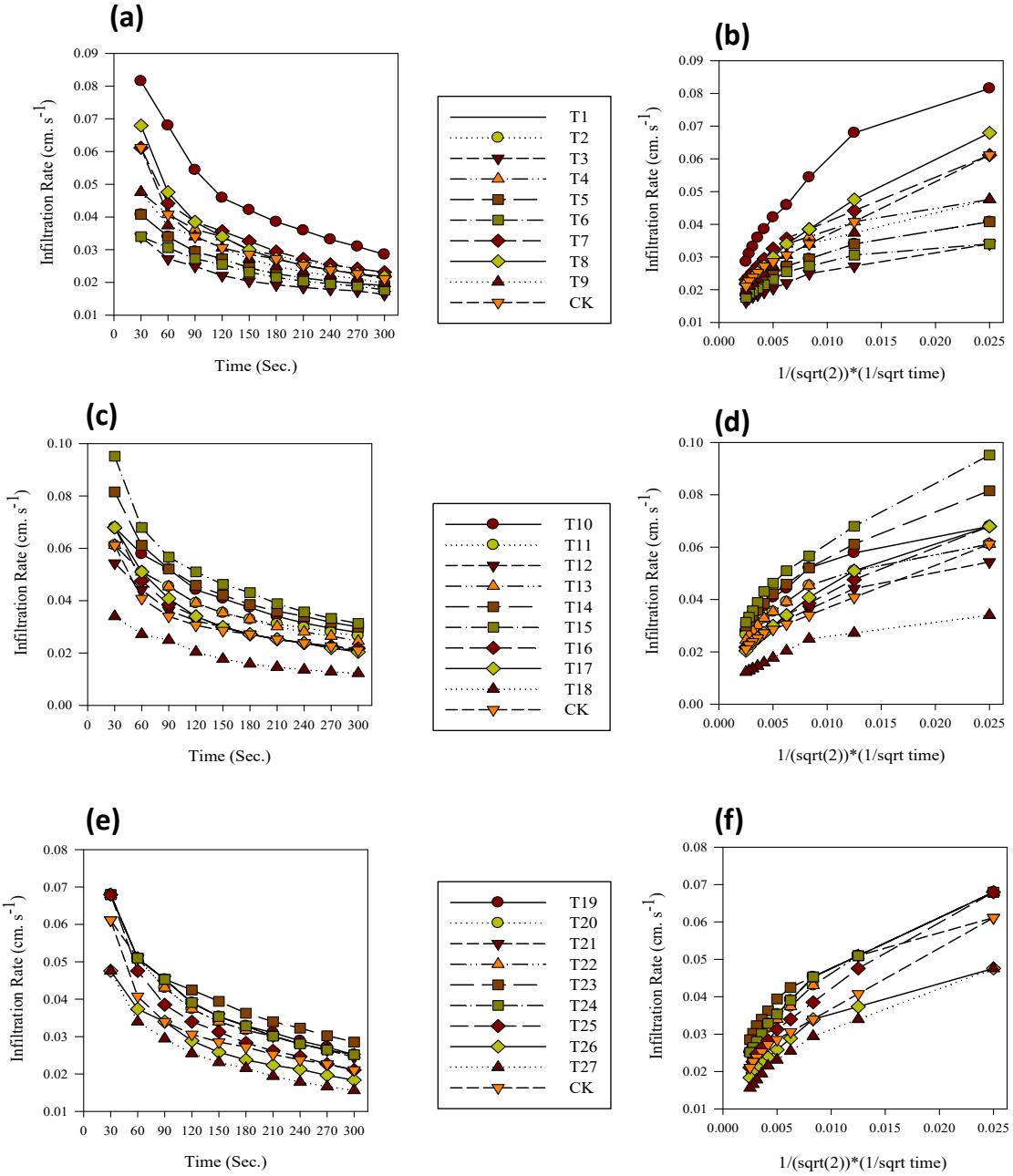



**Figure 8.** Effect of pyrolytic temperature on infiltration rate after wetting after the application of date palm-derived biochar produced at 300 °C ($T_{300}$), 450 °C ($T_{450}$), and 600 °C ($T_{600}$) with particle sizes of 1–2 mm, 0.5–1.0 mm, and less than 0.5 mm ($P_2$, $P_1$, and $P_{0.5}$, respectively), and applied at 1%, 3%, and 5% ($R_1$, $R_3$, and $R_5$, respectively). Panels (**a**,**b**) show the effects of treatments T1 to T9 on the infiltration rate, panels (**c**,**d**) show the effects of treatments T10 to T18 on the infiltration rate, and panels (**e**,**f**) show the effects of treatments T19 to T27 on the infiltration rate (CK: Control, T1: $T_{300}R_1P_2$, T2: $T_{300}R_3P_2$, T3: $T_{300}R_5P_2$, T4: $T_{300}R_1P_1$, T5: $T_{300}R_3P_1$, T6: $T_{300}R_5P_1$, T7: $T_{300}R_1P_{0.5}$, T8: $T_{300}R_3P_{0.5}$, T9: $T_{300}R_5P_{0.5}$, T10: $T_{450}R_1P_2$, T11: $T_{450}R_3P_2$, T12: $T_{450}R_5P_2$, T13: $T_{450}R_1P_1$, T14: $T_{450}R_3P_1$, T15: $T_{450}R_5P_1$, T16: $T_{450}R_1P_{0.5}$, T17: $T_{450}R_3P_{0.5}$, T18: $T_{450}R_5P_{0.5}$, T19: $T_{600}R_1P_2$, T20: $T_{600}R_3P_2$, T21: $T_{600}R_5P_2$, T22: $T_{600}R_1P_1$, T23: $T_{600}R_3P_1$, T24: $T_{600}R_5P_1$, T25: $T_{600}R_1P_{0.5}$, T26: $T_{600}R_3P_{0.5}$, and T27: $T_{600}R_5P_{0.5}$).

### *3.5. Effects on Unsaturated Hydraulic Conductivity*

Prior to immersing the columns in water, the unsaturated hydraulic conductivity was determined. Figure 9 illustrates the unsaturated hydraulic conductivity. All treatments (T2 to T9) showed a substantial decrease in unsaturated hydraulic conductivity ($p < 0.05$). For

biochar produced at 300 °C, a 45.15% to 2.46% decrease was observed after applying T2 to T9 compared to the control. The percentage decrease for biochar produced at 450 °C was 4.48% to 46.50% for T10 to T18. Compared to untreated soil, biochar produced at 600 °C was decreased by 8.60% to 48.24% for T19 to T27. Overall, the highest reduction was found with the highest application rate (5%) and the smallest particle size (0.5 mm) [29]. The reduction in unsaturated hydraulic conductivity could be due to the increase in the diameter of the soil aggregates of biochar-amended soils and subsequent changes in the pore size distribution [13,15].

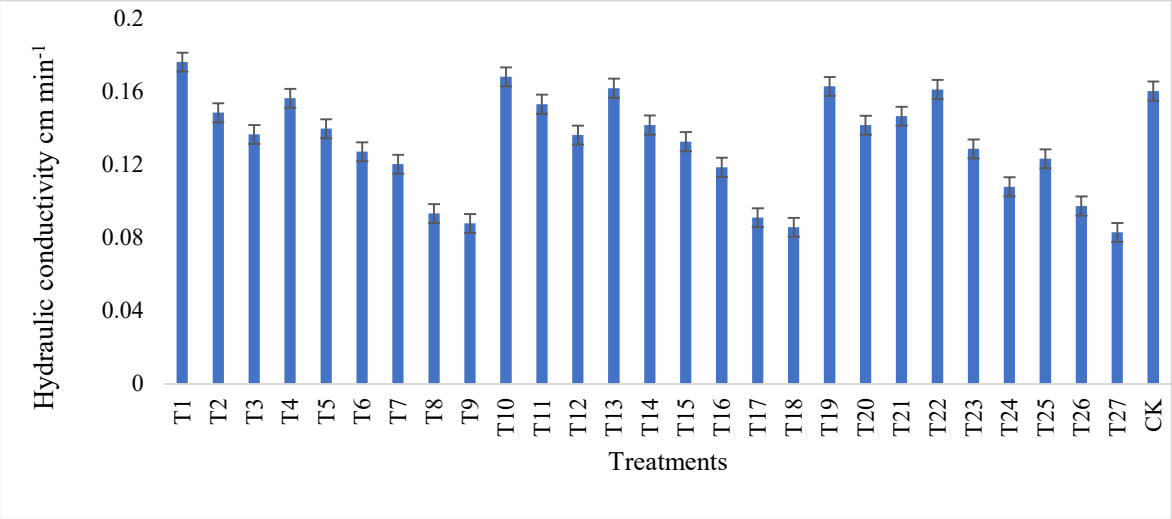



**Figure 9.** Impact of pyrolytic temperature on hydraulic conductivity upon wetness following the application of biochar made from date palms at 300 °C ($T_{300}$), 450 °C ($T_{450}$), and 600 °C ($T_{600}$), with particle sizes of 1–2 mm, 0.5–1.0 mm, and less than 0.5 mm ($P_2$, $P_1$, and $P_{0.5}$, respectively), and applied at 1%, 3%, and 5% ($R_1$, $R_3$, and $R_5$, respectively). (CK: Control, T1: $T_{300}R_1P_2$, T2: $T_{300}R_3P_2$, T3: $T_{300}R_5P_2$, T4: $T_{300}R_1P_1$, T5: $T_{300}R_3P_1$, T6: $T_{300}R_5P_1$, T7: $T_{300}R_1P_{0.5}$, T8: $T_{300}R_3P_{0.5}$, T9: $T_{300}R_5P_{0.5}$, T10: $T_{450}R_1P_2$, T11: $T_{450}R_3P_2$, T12: $T_{450}R_5P_2$, T13: $T_{450}R_1P_1$, T14: $T_{450}R_3P_1$, T15: $T_{450}R_5P_1$, T16: $T_{450}R_1P_{0.5}$, T17: $T_{450}R_3P_{0.5}$, T18: $T_{450}R_5P_{0.5}$, T19: $T_{600}R_1P_2$, T20: $T_{600}R_3P_2$, T21: $T_{600}R_5P_2$, T22: $T_{600}R_1P_1$, T23: $T_{600}R_3P_1$, T24: $T_{600}R_5P_1$, T25: $T_{600}R_1P_{0.5}$, T26: $T_{600}R_3P_{0.5}$, and T27: $T_{600}R_5P_{0.5}$).

Overall, the findings of this study highlighted its potential to significantly enhance water retention and reduce evaporation in arid environments. For farmers, applying biochar at rates of 3% to 5% with smaller particle sizes (e.g., 0.5 mm) can improve soil structure and moisture availability, promoting drought resilience in crops. However, soil testing is recommended to make biochar use effective. Biochar can improve soil quality, as it holds great promise for enhancing agricultural practices in arid environments. For crops in water-scarce environments, its porous nature could aid in increasing soil water retention. Therefore, water resource managers should prioritize educating farmers about the benefits of biochar, support research on local production methods, and integrate biochar use with other water conservation strategies. By implementing these practices, stakeholders can enhance agricultural productivity and promote the sustainable management of water resources in arid regions.

The findings of this research highlight the crucial role of date palm waste-derived biochar in addressing sustainability challenges, especially in arid environments such as Saudi Arabia. The results exhibit that date palm waste-derived biochar can effectively improve soil hydrological characteristics, subsequently enhancing water retention. This research promotes the adoption of biochar in arid agricultural systems, which can enhance crop productivity, while ensuring the sustainable management of water resources.

## 4. Conclusions

Date palm waste-derived biochar was used as an amendment to improve water retention in coarse texture (sandy) soil. The date palm biochar (pyrolyzed at 300 °C, 450 °C, and 600 °C) was ground to different sizes (0.5, 1, and 2 mm) and applied at different rates (1%, 3%, and 5%, *w*/*w*). However, more than 90% of the absorbed water was recovered in most treatments. The application of biochar was found to reduce the unsaturated hydraulic conductivity of soils. Decreases ranged from 2.46% to 45.15% for biochar produced at 300 °C, 4.48% to 46.50% for biochar produced at 450 °C, and 8.60% to 48.24% for biochar produced at 600 °C. Additionally, the rate and volume of water infiltration were reduced by the addition of biochar. The decrease in hydraulic conductivity and infiltration rate is likely due to the filling of macropores and enhanced microporosity caused by the fine particles of biochar. This suggests that the biochar can improve the water-holding capacity of the soil. This study found that application rates of 3% and 5% biochar, with particle sizes of 1 mm and 0.5 mm, effectively improved water retention in the soil. Therefore, date palm waste-derived biochar with a particle size range of 0.5–1 mm and an application rate of 3% could be a suitable soil amendment to improve the hydrological properties of sandy soils in arid and semi-arid regions. Overall, this research demonstrates the potential for biochar, derived from agricultural waste, to be used as a soil conditioner to enhance the water-holding capacity of sandy soils. The findings could have important implications for sustainable land management and crop production in water-limited environments. Future studies on biochar should explore its effects on various soil types, including clay and loamy soils, and conduct long-term field trials to assess its impacts on soil health and crop yield under real-world conditions. The impacts of biochar are particularly significant in arid and semi-arid regions, where sandy soils prevail and water conservation is essential for agricultural productivity. Future studies can be broadened to explore how biochar can provide sustainable solutions for enhancing soil fertility and optimizing water use in agriculture in arid and semi-arid regions of the world.

**Author Contributions:** Conceptualization, A.G.A., A.A. (Abdulrasoul Alomran) and A.A. (Arafat Alkhasha); methodology, A.G.A., A.A. (Abdulrasoul Alomran) and H.M.I. software, A.G.A., A.A. (Abdulrasoul Alomran) and A.A. (Arafat Alkhasha); validation, A.G.A., A.A. (Abdulrasoul Alomran) and Z.A.; formal analysis, A.G.A., A.A. (Abdulrasoul Alomran), Z.A. and A.A. (Arafat Alkhasha); investigation, A.G.A., A.A. (Abdulrasoul Alomran) and H.M.I.; resources, A.G.A.; data curation, A.G.A., A.A. (Abdulrasoul Alomran) and A.A. (Arafat Alkhasha); writing—original draft preparation, A.G.A., A.A. (Abdulrasoul Alomran) and A.A. (Arafat Alkhasha); writing—review and editing, A.G.A., A.A. (Abdulrasoul Alomran), H.M.I., Z.A. and A.A. (Arafat Alkhasha); visualization, A.G.A. and A.A. (Abdulrasoul Alomran); supervision, A.G.A.; project administration, A.G.A.; funding acquisition, A.G.A., H.M.I. and Z.A. All authors have read and agreed to the published version of the manuscript.

**Funding:** Researchers Supporting Project number (RSPD2024R825), King Saud University, Riyadh, Saudi Arabia.

**Institutional Review Board Statement:** Not applicable.

**Informed Consent Statement:** Not applicable.

**Data Availability Statement:** The data are available on request from the authors.

**Acknowledgments:** Researchers Supporting Project number (RSPD2024R825), King Saud University, Riyadh, Saudi Arabia.

**Conflicts of Interest:** The authors declare no conflicts of interest.

## Appendix A

**Table A1.** Linear equations for cumulative infiltration and infiltration rate.

| Treatments | Cumulative Infiltration | | Infiltration Rate | |
|---|---|---|---|---|
| T1 | y = 1.0058x − 0.894 | $R^2$ = 0.9973 | y = 4.9616x + 0.0633 | $R^2$ = 0.9586 |
| T2 | y = 0.8473x − 1.4205 | $R^2$ = 0.9974 | y = 3.2062x + 0.0513 | $R^2$ = 0.9506 |
| T3 | y = 0.7795x − 0.5902 | $R^2$ = 0.9998 | y = 4.0264x + 0.0493 | $R^2$ = 0.9519 |
| T4 | y = 0.8927x − 0.6267 | $R^2$ = 0.9998 | y = 4.7374x + 0.0563 | $R^2$ = 0.9549 |
| T5 | y = 0.7975x − 0.3766 | $R^2$ = 0.9995 | y = 4.6695x + 0.0499 | $R^2$ = 0.967 |
| T6 | y = 0.7255x − 1.1281 | $R^2$ = 0.999 | y = 2.9041x + 0.044 | $R^2$ = 0.9579 |
| T7 | y = 0.6868x − 0.3925 | $R^2$ = 0.9993 | y = 4.0826x + 0.0418 | $R^2$ = 0.9799 |
| T8 | y = 0.5329x − 0.3139 | $R^2$ = 0.9989 | y = 3.0586x + 0.0329 | $R^2$ = 0.9712 |
| T9 | y = 0.502x − 0.815 | $R^2$ = 0.9973 | y = 1.9613x + 0.0303 | $R^2$ = 0.9618 |
| T10 | y = 0.9599x − 0.4124 | $R^2$ = 0.9997 | y = 5.8029x + 0.0594 | $R^2$ = 0.9739 |
| T11 | y = 0.8742x − 0.6113 | $R^2$ = 0.9994 | y = 4.7879x + 0.0543 | $R^2$ = 0.9639 |
| T12 | y = 0.7779x − 0.9345 | $R^2$ = 0.9993 | y = 3.2094x + 0.0499 | $R^2$ = 0.9167 |
| T13 | y = 0.9241x − 0.5621 | $R^2$ = 0.9995 | y = 5.0549x + 0.0584 | $R^2$ = 0.959 |
| T14 | y = 0.8092x − 0.8346 | $R^2$ = 0.9994 | y = 3.9619x + 0.0498 | $R^2$ = 0.9621 |
| T15 | y = 0.7571x − 0.9828 | $R^2$ = 0.9997 | y = 3.1357x + 0.0476 | $R^2$ = 0.9294 |
| T16 | y = 0.6772x − 0.1256 | $R^2$ = 0.9986 | y = 4.5397x + 0.0413 | $R^2$ = 0.9805 |
| T17 | y = 0.5199x − 0.4745 | $R^2$ = 0.9987 | y = 2.81x + 0.0312 | $R^2$ = 0.9813 |
| T18 | y = 0.4896x − 0.4489 | $R^2$ = 0.9992 | y = 2.3431x + 0.0311 | $R^2$ = 0.9384 |
| T19 | y = 0.9299x − 0.2534 | $R^2$ = 0.9989 | y = 6.133x + 0.0563 | $R^2$ = 0.9846 |
| T20 | y = 0.8089x − 0.2058 | $R^2$ = 0.9996 | y = 5.1965x + 0.0499 | $R^2$ = 0.9763 |
| T21 | y = 0.8365x − 1.6043 | $R^2$ = 0.9991 | y = 2.6263x + 0.0513 | $R^2$ = 0.9284 |
| T22 | y = 0.9201x − 0.4812 | $R^2$ = 0.9992 | y = 5.6107x + 0.0556 | $R^2$ = 0.9827 |
| T23 | y = 0.7345x − 0.219 | $R^2$ = 0.9997 | y = 4.6619x + 0.0453 | $R^2$ = 0.9775 |
| T24 | y = 0.6161x + 0.1208 | $R^2$ = 0.9989 | y = 4.5033x + 0.0381 | $R^2$ = 0.9834 |
| T25 | y = 0.7039x − 0.272 | $R^2$ = 0.9989 | y = 4.4693x + 0.0427 | $R^2$ = 0.9818 |
| T26 | y = 0.5562x − 0.5139 | $R^2$ = 0.9993 | y = 2.8757x + 0.0341 | $R^2$ = 0.9687 |
| T27 | y = 0.4737x − 0.4182 | $R^2$ = 0.9993 | y = 2.5115x + 0.0289 | $R^2$ = 0.9728 |
| CK | y = 0.9152x − 0.5674 | $R^2$ = 0.9993 | y = 5.1216x + 0.0571 | $R^2$ = 0.9617 |

## References


1. Yost, J.L.; Hartemink, A.E. Soil organic carbon in sandy soils: A review. *Adv. Agron.* **2019**, *158*, 217–310.
2. Osman, K.T. Sandy soils. In *Management of Soil Problems*; Springer: Berlin/Heidelberg, Germany, 2018; pp. 37–65.
3. Weber, J.; Karczewska, A.; Drozd, J.; Licznar, M.; Licznar, S.; Jamroz, E.; Kocowicz, A. Agricultural and ecological aspects of a sandy soil as affected by the application of municipal solid waste composts. *Soil Biol. Biochem.* **2007**, *39*, 1294–1302. [CrossRef]
4. Alghamdi, A.G. Biochar as a potential soil additive for improving soil physical properties—A review. *Arab. J. Geosci.* **2018**, *11*, 766. [CrossRef]
5. Atkinson, C.J.; Fitzgerald, J.D.; Hipps, N.A. Potential mechanisms for achieving agricultural benefits from biochar application to temperate soils: A review. *Plant Soil* **2010**, *337*, 1–18. [CrossRef]
6. Gluba, L.; Rafalska-Przysucha, A.; Szewczak, K.; Lukowski, M.; Szlazak, R.; Vitkova, J.; Kobylecki, R.; Bis, Z.; Wichlinski, M.; Zarzycki, R.; et al. Effect of Fine Size-Fractionated Sunflower Husk Biochar on Water Retention Properties of Arable Sandy Soil. *Materials* **2021**, *14*, 1335. [CrossRef]

7. Alghamdi, A.G.; Aljohani, B.H.; Aly, A.A. Impacts of Olive Waste-Derived Biochar on Hydro-Physical Properties of Sandy Soil. *Sustainability* **2021**, *13*, 5493. [CrossRef]
8. Bordoloi, S.; Kumar, H.; Hussain, R.; Karangat, R.; Lin, P.; Sreedeep, S.; Zhu, H.-H. Assessment of hydro-mechanical properties of biochar-amended soil sourced from two contrasting feedstock. *Biomass Convers. Biorefinery* **2020**, *14*, 5803–5818. [CrossRef]
9. Garcia-Perez, T.; Pelaez-Samaniego, M.R.; Delgado-Noboa, J.; Chica, E.J. Combined Effect of Biochar and Fertilizers on Andean Highland Soils before and after Cropping. *Sustainability* **2022**, *14*, 8912. [CrossRef]
10. Loaiza, J.G.; Bustos-Terrones, Y.; Bustos-Terrones, V.; Monjardín-Armenta, S.A.; Quevedo-Castro, A.; Estrada-Vazquez, R.; Rangel-Peraza, J.G. Evaluation of the Hydrochemical and Water Quality Characteristics of an Aquifer Located in an Urbanized Area. *Appl. Sci.* **2022**, *12*, 6879. [CrossRef]
11. Baiamonte, G.; Crescimanno, G.; Parrino, F.; De Pasquale, C. Effect of biochar on the physical and structural properties of a sandy soil. *Catena* **2019**, *175*, 294–303. [CrossRef]
12. Ahmad Bhat, S.; Kuriqi, A.; Dar, M.U.D.; Bhat, O.; Sammen, S.S.; Towfiqul Islam, A.R.M.; Elbeltagi, A.; Shah, O.; Ai-Ansari, N.; Ali, R.; et al. Application of Biochar for Improving Physical, Chemical, and Hydrological Soil Properties: A Systematic Review. *Sustainability* **2022**, *14*, 11104. [CrossRef]
13. Alkharabsheh, H.M.; Seleiman, M.F.; Battaglia, M.L.; Shami, A.; Jalal, R.S.; Alhammad, B.A.; Almutairi, K.F.; Al-Saif, A.M. Biochar and Its Broad Impacts in Soil Quality and Fertility, Nutrient Leaching and Crop Productivity: A Review. *Agronomy* **2021**, *11*, 993. [CrossRef]
14. Hussain, R.; Kumar, G.K.; Ravi, K. Impact of biochar produced from hardwood of mesquite on the hydraulic and physical properties of compacted soils for potential application in engineered structures. *Geoderma* **2021**, *385*, 114836. [CrossRef]
15. Yan, Y.; Nakhli, S.A.A.; Jin, J.; Mills, G.; Willson, C.S.; Legates, D.R.; Manahiloh, K.N.; Imhoff, P.T. Predicting the impact of biochar on the saturated hydraulic conductivity of natural and engineered media. *J. Environ. Manag.* **2021**, *295*, 113143. [CrossRef]
16. Alghamdi, A.G.; Alkhasha, A.; Ibrahim, H.M. Effect of biochar particle size on water retention and availability in a sandy loam soil. *J. Saudi Chem. Soc.* **2020**, *24*, 1042–1050. [CrossRef]
17. Al-Omran, A.M.; Ibrahim, A.; Alharbi, A.R. Effects of Biochar and Compost on Soil Physical Quality Indices. *Commun. Soil Sci. Plant Anal.* **2021**, *52*, 2482–2499. [CrossRef]
18. Günal, E.; Erdem, H.; Çelik, İ. Effects of three different biochar amendments on water retention of silty loam and loamy soils. *Agric. Water Manag.* **2018**, *208*, 232–244. [CrossRef]
19. Wang, K.; Zhang, X.; Sun, C.; Yang, K.; Zheng, J.; Zhou, J. Biochar application alters soil structure but not soil hydraulic conductivity of an expansive clayey soil under field conditions. *J. Soils Sediments* **2021**, *21*, 73–82. [CrossRef]
20. Alkhasha, A.; Al-Omran, A.; Aly, A. Effects of Biochar and Synthetic Polymer on the Hydro-Physical Properties of Sandy Soils. *Sustainability* **2018**, *10*, 4642. [CrossRef]
21. Toková, L.; Igaz, D.; Horák, J.; Aydin, E. Effect of Biochar Application and Re-application on Soil Bulk Density, Porosity, Saturated Hydraulic Conductivity, Water Content and Soil Water Availability in a Silty Loam Haplic Luvisol. *Agronomy* **2020**, *10*, 1005. [CrossRef]
22. Ayaz, M.; Feiziene, D.; Feiza, V.; Tilvikiene, V.; Baltrenaite-Gediene, E.; Khan, A. The Impact of Swine Manure Biochar on the Physical Properties and Microbial Activity of Loamy Soils. *Plants* **2022**, *11*, 1729. [CrossRef] [PubMed]
23. Gee, G.W.; Bauder, J.W. Particle-size analysis. In *Methods of Soil Analysis, Part 1: Physical and Mineralogical Methods. Agronomy Monograph No. 9*, 2nd ed.; Klute, A., Ed.; American Society of Agronomy; Soil Science Society of America: Madison, WI, USA, 1986; pp. 383–411.
24. Richard, L.A. Diagnosis and improvement of saline and alkali soils. In *USDA Book HandBook. No. 60*; US Department of Agriculture: Washington, DC, USA, 1954; p. 160.
25. Faloye, O.; Ajayi, E.; Rostek, J.; Babalola, T.; Fashina, A.; Horn, R. Water hydraulics, retention, and repellency; response to soil texture, biochar pyrolysis conditions and wetting/drying. *Int. Agrophys.* **2022**, *36*, 155–163. [CrossRef]
26. Walkley, A.; Black, I.A. An examination of Degtjareff method for determining soil organic matter and a proposed modification of the chromic acid titration method. *Soil Sci.* **1934**, *37*, 29–38. [CrossRef]
27. Sparks, D.L.; Page, A.L.; Helmke, P.A.; Loeppert, R.H. (Eds.) *Methods of Soil Analysis, Part 3: Chemical Methods*; John Wiley & Sons: Hoboken, NJ, USA, 2020; Volume 14.
28. Philip, J.R. Theory of infiltration. In *Advances in Hydroscience*; Elsevier: Amsterdam, The Netherlands, 1969; Volume 5, pp. 215–296.
29. Alghamdi, A.G.; Al-Omran, A.; Alkhasha, A.; Alasmary, Z.; Aly, A.A. Significance of Pyrolytic Temperature, Particle Size, and Application Rate of Biochar in Improving Hydro-Physical Properties of Calcareous Sandy Soil. *Agriculture* **2021**, *11*, 1293. [CrossRef]
30. Adekiya, A.O.; Agbede, T.M.; Olayanju, A.; Ejue, W.S.; Adekanye, T.A.; Adenusi, T.T.; Ayeni, J.F. Effect of biochar on soil properties, soil loss, and cocoyam yield on a tropical sandy loam Alfisol. *Sci. World J.* **2020**, *2020*, 9391630. [CrossRef]
31. Obia, A.; Mulder, J.; Martinsen, V.; Cornelissen, G.; Børresen, T. In situ effects of biochar on aggregation, water retention and porosity in light-textured tropical soils. *Soil Tillage Res.* **2016**, *155*, 35–44. [CrossRef]
32. Gelardi, D.L.; Ainuddin, I.H.; Rippner, D.A.; Patiño, J.E.; Abou Najm, M.; Parikh, S.J. Biochar alters hydraulic conductivity and impacts nutrient leaching in two agricultural soils. *Soil* **2021**, *7*, 811–825. [CrossRef]
33. Al-Omran, A.M.; Ibrahim, A.; Alharbi, A.R. Evaluating the Impact of Combined Application of Biochar and Compost on Hydro-physical Properties of Sandy Soil. *Commun. Soil Sci. Plant Anal.* **2019**, *50*, 2442–2456. [CrossRef]

34. Lu, Y.; Gu, K.; Shen, Z.; Wang, X.; Zhang, Y.; Tang, C.S.; Shi, B. Effects of biochar particle size and dosage on the desiccation cracking behavior of a silty clay. *Sci. Total Environ.* **2022**, *837*, 155788. [CrossRef] [PubMed]
35. Šimanský, V.; Horák, J.; Bordoloi, S. Improving the soil physical properties and relationships between soil properties in arable soils of contrasting texture enhancement using biochar substrates: A case study in Slovakia. *Geoderma Reg.* **2022**, *28*, e00443. [CrossRef]
36. Sun, F.; Lu, S. Biochars improve aggregate stability, water retention, and pore-space properties of clayey soil. *J. Plant Nutr. Soil Sci.* **2014**, *177*, 26–33. [CrossRef]
37. Alkhasha, A.; Al-Omran, A. Evaluating the effects of biochar and SAP polymer on soil physical quality indices. *Commun. Soil Sci. Plant Anal.* **2020**, *51*, 1123–1135. [CrossRef]
38. Duan, M.; Liu, G.; Zhou, B.; Chen, X.; Wang, Q.; Zhu, H.; Li, Z. Effects of modified biochar on water and salt distribution and water-stable macro-aggregates in saline-alkaline soil. *J. Soils Sediments* **2021**, *21*, 2192–2202. [CrossRef]
39. Razzaghi, F.; Obour, P.B.; Arthur, E. Does biochar improve soil water retention? A systematic review and meta-analysis. *Geoderma* **2020**, *361*, 114055. [CrossRef]
40. Sharma, P.; Abrol, V.; Sharma, V.; Chaddha, S.; Srinivasa Rao, C.; Ganie, A.Q.; Ingo Hefft, D.; El-Sheikh, M.A.; Mansoor, S. Effectiveness of biochar and compost on improving soil hydro-physical properties, crop yield and monetary returns in inceptisol subtropics. *Saudi J. Biol. Sci.* **2021**, *28*, 7539–7549. [CrossRef] [PubMed]


**Disclaimer/Publisher's Note:** The statements, opinions and data contained in all publications are solely those of the individual author(s) and contributor(s) and not of MDPI and/or the editor(s). MDPI and/or the editor(s) disclaim responsibility for any injury to people or property resulting from any ideas, methods, instructions or products referred to in the content.